J Shoulder Elbow Surg (2021) 30, 1152–1158

ELSEVIER

Journal of Shoulder and Elbow Surgery

www.elsevier.com/locate/ymse

Utility of a 3-dimensionally printed color-coded bone model to visualize impinging osteophytes for arthroscopic débridement arthroplasty in elbow osteoarthritis

Atsuo Shigi, MD[a], Kunihiro Oka, MD[b,*], Hiroyuki Tanaka, MD[b], Ryoya Shiode, MD[b], Tsuyoshi Murase, MD[b]

[a]*Yukioka Hospital Hand Center, Osaka, Japan*
[b]*Department of Orthopaedic Surgery, Graduate School of Medicine, Osaka University, Suita, Japan*

Background: The identification and precise removal of bony impingement lesions during arthroscopic débridement arthroplasty for elbow osteoarthritis require a high level of experience and surgical skill. We have developed a new technique to identify impinging osteophytes on a computer display by simulating elbow motion using the multiple positions of 3-dimensional (3D) elbow models created from computed tomography data. Moreover, an actual color-coded 3D model indicating the impinging osteophytes was created with a 3D printer and was used as an intraoperative reference tool. This study aimed to verify the efficacy of these new technologies in arthroscopic débridement for elbow osteoarthritis.

Methods: We retrospectively studied 16 patients treated with arthroscopic débridement for elbow osteoarthritis after a preoperative computer simulation. Patients who underwent surgery with only the preoperative simulation were assigned to group 1 (n = 8), whereas those on whom we operated using a color-coded 3D bone model created from the preoperative simulation were assigned to group 2 (n = 8). Elbow extension and flexion range of motion (ROM), the Mayo Elbow Performance Score (MEPS), and the severity of osteoarthritis were compared between the groups.

Results: Although preoperative elbow flexion and MEPS values were not significantly different between the groups, preoperative extension was significantly more restricted in group 2 than in group 1 ($P = .0131$). Group 2 tended to include more severe cases according to the Hastings-Rettig classification ($P = .0693$). ROM and MEPS values were improved in all cases. No significant differences in postoperative ROM or MEPS values were observed between the groups. There were no significant differences in the improvement in ROM or MEPS values between the 2 groups.

Conclusions: The use of preoperative simulation and a color-coded bone model could help to achieve as good postoperative ROM and MEPS values for advanced elbow osteoarthritis as those for early and intermediate stages.

Level of evidence: Level III; Retrospective Cohort Comparison; Treatment Study

Keywords: Color-coded 3-dimensional model; computer simulation; elbow arthroscopy; osteoarthritis; débridement arthroplasty; 3-dimensional printer

This study was approved by the Institutional Review Board of the Academic Clinical Research Center of Osaka University (approval no. 09157-4) and followed the tenets of the Declaration of Helsinki (as revised in 2000). Each author certifies that his or her institution approved the human protocol for this investigation, all investigations were conducted in conformity with ethical principles of research, and informed consent was obtained from all study participants.

*Reprint requests: Kunihiro Oka, MD, Department of Orthopaedic Surgery, Graduate School of Medicine, Osaka University, 2-2, Yamadaoka, Suita, Osaka 565-0871, Japan.

E-mail address: oka-kunihiro@umin.ac.jp (K. Oka).

1058-2746/$ - see front matter
https://doi.org/10.1016/j.jse.2020.12.002

For symptomatic osteoarthritis of the elbow joint with restricted range of motion (ROM) and pain, débridement arthroplasty, which includes excision of impinging osteophytes, synovectomy, and capsular release, has been performed.[3,18,28,32,33] Recently, the arthroscopic technique has become popular owing to its lower invasiveness compared with conventional open arthroplasty.[1,2,5,10-12,20,31] However, the limited arthroscopic field of view coupled with the complex elbow anatomy and the narrow intracapsular space due to capsular contracture and synovial fibrosis makes the operation difficult, such that it requires a high level of experience and surgical skill. The arthroscopic technique depends mostly on the surgeon's ability to recognize the impinging osteophytes that cause restricted joint motion. Furthermore, an unnecessary amount of resection could lead to additional invasiveness and, even more important, instability of the elbow.[9]

For these reasons, we have developed a new technique to identify and visualize the impinging osteophytes on a computer display by simulating the flexion-extension motion of the elbow joint with the use of 3-dimensional (3D) virtual bone models created from computed tomography (CT) data[16] and an in vivo 3D kinematic technique enabled by the recent image analysis.[6,7,15] Using this technique, a surgeon can resect the osteophytes during the arthroscopic procedure while referring to the images on the display generated by the preoperative simulation but still relying on his or her subjective estimation intraoperatively. Thus, a reference guide to reflect the preoperative simulation in the actual surgical procedure would be of great help for surgeons to perform the operation as accurately as it was planned. We have also used a 3D printer, which is a technology that has recently been applied in some areas of surgery. A recently developed 3D printer can create a real-sized model of a human organ that is color coded for each anatomic part, using several types of material of various colors. With this function of the 3D printer, in combination with a preoperative simulation, we can produce a bone model showing the impinging osteophytes to be removed in a different color from the other osteophytes. During the actual surgical procedure, the surgeon should be able to remove the impinging osteophytes more easily, more efficiently, and less invasively by using the color-coded 3D model as a reference. In this study, we investigated the feasibility and efficacy of the color-coded 3D resin bone model as an intraoperative reference tool for arthroscopic arthroplasty for osteoarthritis of the elbow joint.

Materials and methods

This was a retrospective case-control study on arthroscopic débridement using a color-coded 3D resin bone model for marking impinging osteophytes for elbow osteoarthritis. Sixteen patients who underwent arthroscopic débridement for elbow osteoarthritis after a preoperative computer simulation between February 2010 and October 2018 participated in the investigation. We categorized the 16 patients into 2 groups. Patients who underwent surgery with only the preoperative simulation were assigned to group 1 (n = 8), whereas those on whom we operated using a color-coded 3D bone model created from the preoperative simulation were assigned to group 2 (n = 8). Our institution used only the preoperative simulation until July 2014; the additional color-coded 3D bone model has been used since August 2014.

CT data on the elbow joint were obtained in 3 different positions (maximum flexion, 90°, and maximum extension) using a low–radiation dose protocol (slice thickness, 1.25 mm; scan time, 0.5 seconds; scan pitch, 0.562:1; tube current, 10-30 mA; tube voltage, 120 kV) (LightSpeed Ultra 16; General Electric, Waukesha, WI, USA) while the forearm was maintained in neutral rotation.[15] Digital data (Digital Imaging and Communications in Medicine format) were sent to a computer (Precision T5500; Dell, Round Rock, TX, USA), and 3D models of the humerus, ulna, and radius were created using a dedicated computer program (Bone Viewer; Orthree, Osaka, Japan) (Fig. 1, *A*). The 3D models of the humerus at various elbow flexion angles were semiautomatically superimposed on the simulation software using a 3D surface registration technique (Bone Simulator; Orthree), and the relative positions of the ulnae were determined. A previous study evaluated the accuracy of the 3D registration technique: The rotation error was 0.38° ± 0.62°, and the translation error was 0.56 ± 0.06 mm.[21] According to the previously reported methods, we calculated 2 rotational axes of the elbow using the screw-displacement axis technique.[6,7,15,16] The axis from 90° to maximum flexion was defined as the flexion axis, whereas that from 90° to maximum extension was defined as the extension axis. We rotated the forearm bones around the flexion axis until the elbow flexed 140° and rotated them around the extension axis until the elbow extended 0°. The overlapping regions between the humerus and the forearm bones at 140° of flexion and at 0° of extension were considered impinging osteophytes (Fig. 1, *B*). The impinging osteophytes were then quantified and visualized 3-dimensionally on the computer (Fig. 2).[16] It took about 90 minutes to create 3D models and identify the impinging lesions on the computer simulation. The operator transferred the 3D data to a 3D printer (Connex 3 Objet 350; Stratasys, Eden Prairie, MN, USA) and prepared modeling (within 10 minutes). The color-coded 3D bone model was shaped automatically (Fig. 3). The bony structures that did not influence elbow ROM were composed of translucent yellow acrylic resin (Objet FullCure 720; Stratasys) whereas the impinging osteophytes were composed of solid white acrylic compounds (Objet VeroWhitePlus RGD 835; Stratasys) so that one could easily recognize the bony parts to remove during surgery. The lamination thickness of the 3D printer was 0.03 mm. The cost of a color-coded bone model was about $500.

Three hand surgeons with sufficient surgical experience conducted arthroscopic débridement in all cases. Under general anesthesia, the patient was placed in the prone position and the upper arm was kept on a holder with the shoulder abducted 90°, the elbow flexed 90°, and the forearm dropped downward. After the elbow had been instilled with 20 to 30 mL of saline solution, we created the anteromedial portal and then the anterolateral portal. We performed débridement arthroplasty on the anterior side of the elbow joint prior to débriding the posterior side. We then created the posterior, posterolateral, and direct lateral portals for the posterior side of the elbow joint. After removing the

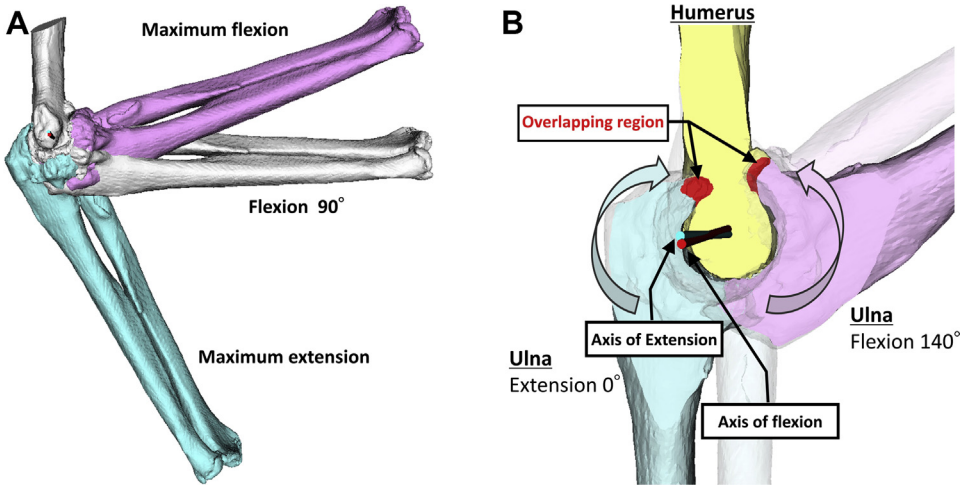

Figure 1 Preoperative simulation to identify impinging lesion. (**A**) Three-dimensional bone model of humerus, ulna, and radius in maximum flexion, 90° of flexion, and maximum extension. (**B**) Sagittal cross-sectional view of elbow simulating 140° of flexion around the flexion axis and 0° of extension around the extension axis. The overlapping region *(red)* was visualized as the impinging lesion.

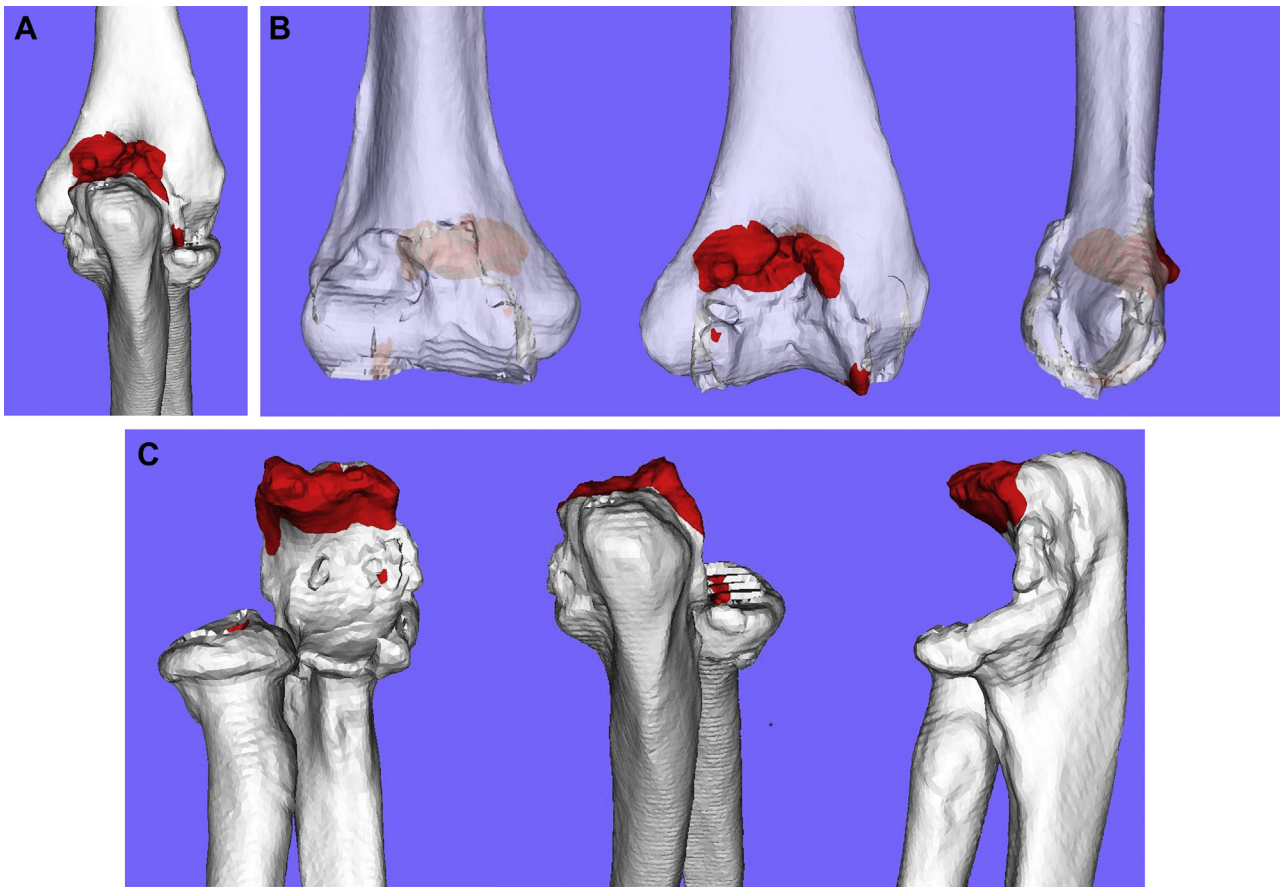

Figure 2 Three-dimensional computer model of elbow, including impinging osteophyte *(red)*. (**A**) Posterior view of elbow. (**B**) Anterior, posterior, and medial views of humerus. (**C**) Anterior, posterior, and medial views of ulna and radius.

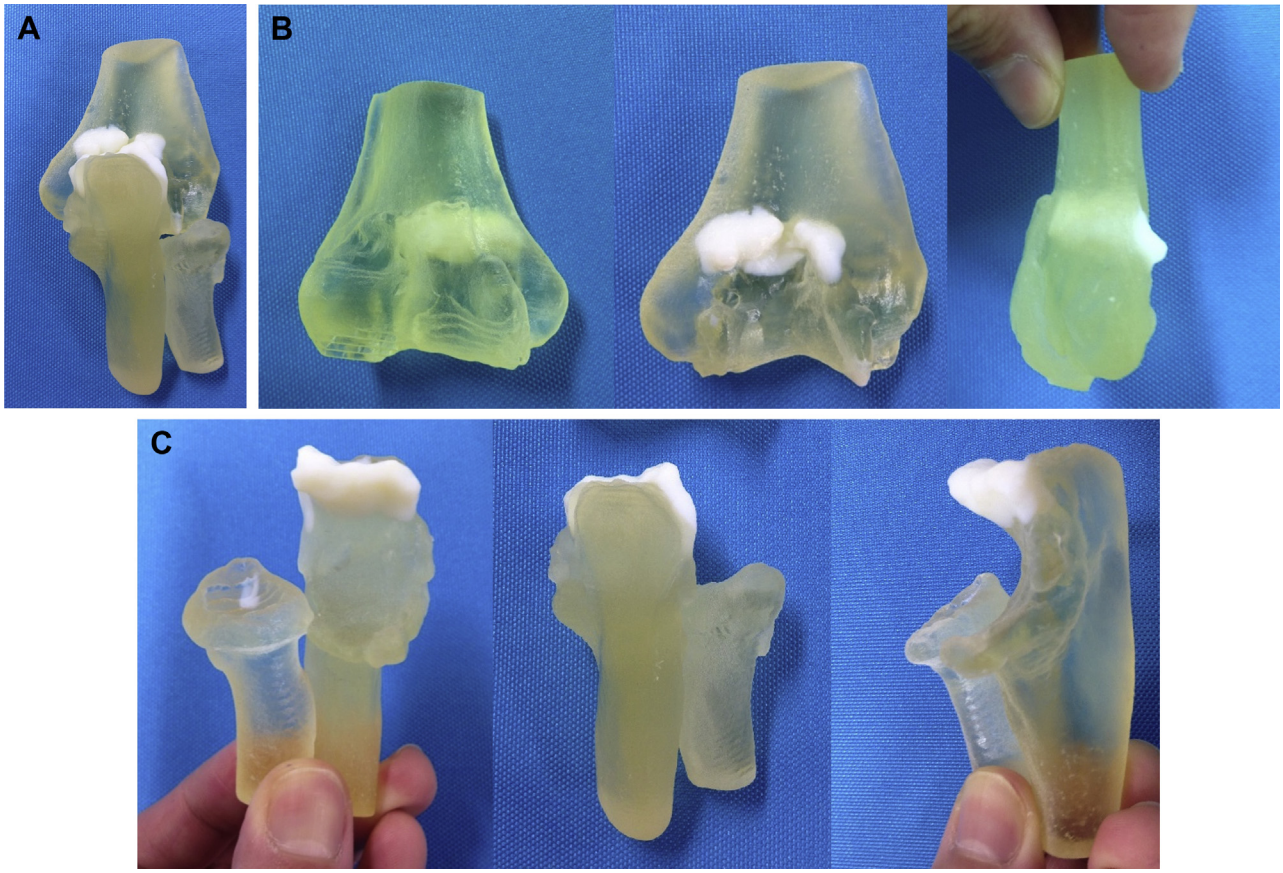

Figure 3 Color-coded bone model of elbow, including impinging osteophyte *(white)*. (**A**) Posterior view of elbow. (**B**) Anterior, posterior, and lateral views of humerus. (**C**) Anterior, posterior, and medial views of ulna and radius.

proliferated synovium, synovial fibrosis, and loose bodies, we resected the impinging osteophytes while referring to the simulation results displayed on the computer monitor (group 1) or using the color-coded 3D bone model that was sterilized and brought into the surgical field (group 2). In patients who had ulnar nerve symptoms or severe preoperative ROM restriction (extension $< -60°$ and flexion $< 100°$), ulnar nerve transposition and release of the posterior oblique ligament of the medial collateral ligament were added to the arthroscopic procedure (5 cases in group 1 and 4 cases in group 2).[3] Mild ROM exercises began on 1 day postoperatively under the supervision of a physiotherapist. Rehabilitation continued until the ROM of the elbow reached a plateau.

We obtained clinical data from the medical records, including operation time; extension and flexion ROM before the operation, at the operation, and at the 1-year follow-up evaluation; and the Mayo Elbow Performance Score (MEPS) preoperatively and at the 1-year follow-up evaluation. The surgeons' opinion toward the usefulness of the color-coded model was rated using 5 grades: 1, very useful; 2, useful; 3, neutral; 4, less useful; and 5, not useful. The preoperative severity of osteoarthritis was assessed by the Hastings-Rettig classification using a plain radiograph.[27] The measurements and scores were compared between the groups.

Statistical analysis

Normality was tested using the Shapiro-Wilk test for continuous variables. We used the Fisher exact test for the analysis of categorical variables. For data with a normal distribution, we used a paired t test to compare preoperative with postoperative data or an unpaired t test to compare group 1 with group 2, and the data are presented as average $\pm$ standard deviation. When the data were not normally distributed, the Wilcoxon signed rank test or Mann-Whitney U test was used, and data are shown as median (interquartile range [IQR]). $P < .05$ was considered statistically significant.

Results

The details of the preoperative and postoperative patient data are shown in Tables I and II, respectively. The age at surgery was significantly higher in group 2 than in group 1 ($P = .0208$). Although preoperative elbow flexion and MEPS values were not significantly different between the groups, preoperative extension was significantly more

Table I Preoperative data in group 1 (computer simulation only) vs. group 2 (computer simulation plus color-coded model)

Preoperative data	Group 1	Group 2	*P* value
Sex			.4667*
Male	8	6	
Female	0	2	
Affected side			>.9999*
Dominant	7	7	
Nondominant	1	1	
Age, median (IQR), yr	47 (31-64)	71 (64-73)	.0208†
Hastings-Rettig classification			.0693†
I	4	0	
II	3	2	
III	1	3	
ROM, mean ± SD, °			
Flexion	114 ± 14	118 ± 13	.6486‡
Extension	−19 ± 6	−29 ± 7	.0131‡
MEPS, median (IQR)	67.5 (60.0-71.3)	65.0 (58.8-70.0)	.5943†

IQR, interquartile range; *ROM*, range of motion; *SD*, standard deviation; *MEPS*, Mayo Elbow Performance Score.
* Fisher exact test.
† Mann-Whitney *U* test.
‡ Unpaired *t* test.

restricted in group 2 than in group 1 ($P = .0131$). Group 2 tended to include more severe cases according to the Hastings-Rettig classification ($P = .0693$). There was no significant difference in the other preoperative background data.

We did not find significant differences in the operation time and ROM at operation between groups 1 and 2. The follow-up term in group 1 and group 2 was 360 ± 60 days and 335 ± 90 days, respectively ($P = .5978$). ROM and MEPS values at 1 year showed improvement in all cases. In group 1, mean extension improved from −19° ± 6° preoperatively to −13° ± 13° postoperatively ($P = .1803$) and mean flexion significantly improved from 114° ± 14° preoperatively to 127° ± 8° postoperatively ($P = .0095$). In group 2, mean extension and mean flexion significantly improved from −29° ± 7° preoperatively to −13° ± 10° postoperatively ($P = .0001$) and from 118° ± 13° preoperatively to 129° ± 9° postoperatively ($P = .014$), respectively. No significant difference in postoperative ROM was observed between the groups. The improvement in extension in group 2 (16° ± 6°) tended to be greater than that in group 1 (6° ± 12°, $P = .0633$). The MEPS significantly improved from 67.5 (IQR, 60.0-71.3) preoperatively to 100 (IQR, 85.0-100.0) postoperatively in group 1 ($P = .0009$) and from 65.0 (IQR, 58.8-70.0) preoperatively to 97.5 (IQR, 85.0-100.0) postoperatively in group 2 ($P = .0008$). There were no significant differences in ROM or MEPS improvement between the 2 groups. The usefulness of the color-coded model was rated 1 in 4 cases and 2 in 4 cases. No cases were rated 3-5. Cases with poor preoperative ROM (extension-flexion arc < 90°) were rated as 1 by the surgeons.

Discussion

Osteoarthritis of the elbow often develops in middle-aged physical laborers and athletes.[30] Typical symptoms are pain at the endpoints of movement, restricted elbow ROM, and a catching and locking sensation.[3,18] Radiographically, osteophyte formation and loose bodies are typically observed at the coronoid and olecranon fossae whereas the ulnohumeral joint is relatively preserved.[4,27] Therefore,

Table II Postoperative results in group 1 (computer simulation only) vs. group 2 (computer simulation plus color-coded model)

Preoperative data	Group 1	Group 2	*P* value
Operation time, median (IQR), min	138 (127-155)	141 (133-169)	.5640*
ROM at operation, mean ± SD, °			
Flexion	131 ± 9	128 ± 4	.3820†
Extension	−5 ± 7	−8 ± 11	.5120†
ROM at 1 yr, mean ± SD, °			
Flexion	127 ± 8	129 ± 9	.5848†
Extension	−13 ± 13	−13 ± 10	>.9999†
MEPS, median (IQR)	100.0 (85.0-100.0)	97.5 (85.0-100.0)	.9530*
Δ ROM, mean ± SD, °			
Flexion	13 ± 10	12 ± 10	.9039†
Extension	6 ± 12	16 ± 6	.0633†
Δ MEPS, median (IQR)	27.5 (23.8-30.0)	30.0 (27.5-35.0)	.2775*

IQR, interquartile range; *ROM*, range of motion; *SD*, standard deviation; *MEPS*, Mayo Elbow Performance Score; *Δ*, change from preoperatively to postoperatively.
* Mann-Whitney *U* test.
† Unpaired *t* test.

débridement arthroplasty that involves synovectomy, capsular release, loose body removal, and resection of impinging osteophytes has been performed for mild and moderate elbow osteoarthritis with favorable clinical outcomes in terms of pain relief and ROM improvement.[3,18,28,32,33] Débridement arthroplasty, which used to be performed by a conventional open method, has increasingly been performed less invasively using arthroscopy.[1,2,5,24]

Before performing an arthroscopic elbow débridement, the surgeon estimates which osteophytes to remove based on observing them on plain radiographs and CT images. During the actual operation, he or she removes the impinging osteophytes while confirming intra-articular impingement during elbow flexion and extension. However, it is not easy to remove all the impinging osteophytes while minimizing unnecessary resection, which can lead to longer surgical times, swelling, invasiveness, and possible joint instability. Thus, considerable surgical skill and experience are required to identify and precisely remove the impinging osteophytes intraoperatively. Hence, we developed a preoperative computer simulation technique to identify impinging osteophytes that require removal to achieve nearly normal elbow ROM.[16] Our procedure simulates in vivo flexion-extension elbow motion with the use of 3D bone models on a computer to help surgeons identify impinging osteophytes and enable their efficient débridement. Furthermore, we introduced a color-coded 3D bone model as a reference, which helps surgeons to conduct surgery more easily by indicating the part to remove with a specific color.

A color-coded 3D model could assist 3D surgical manipulation by intraoperatively presenting the part to remove. In the field of orthopedic surgery, a single-colored 3-dimensionally printed model has been used as an operative planning and intraoperative reference tool.[14,17,19,22,23,25,35] In the field of abdominal surgery, colored 3D printing technology has been used to confirm the position of tumors and vascular anatomy during surgical procedures such as liver resection and transplantation.[8,26,34] Therefore, we focused on the color-coded 3D bone model, which can express the region of interest using multiple colors for arthroscopic débridement arthroplasty of the elbow joint. By observing and touching the impinging lesion as shown in a specific color in a life-sized 3D model, it is much easier to identify the impinging lesion.

In this study, there was no significant difference in operation time between group 1 and group 2. We expected a reduction in the operation time using the color-coded bone model; however, there were other factors besides the resection of osteophytes, such as the resection of fibrous tissue and capsulotomy in cases with severe elbow contractures, as well as additional surgery for ulnar nerve disorders. Although the ROM and MEPS improved in all cases, there was no significant difference between groups 1 and 2 in terms of postoperative results. However, group 2 included more severe cases of extension restriction and more severe cases of osteoarthritis according to the Hastings-Rettig classification than group 1 and included 2 cases with a preoperative elbow arc $< 80^\circ$, which has been reported to be a poor prognostic factor.[13] A systematic review of the clinical results of arthroscopic débridement for elbow osteoarthritis (9 articles; 209 patients; mean age, 45.7 ± 7.1 years) showed improvement in elbow extension (from -23.4° to -10.7°), flexion (from 115.9° to 128.7°), and the MEPS (from 60.7 to 84.6).[29] Our study showed equivalent ROM and higher MEPS values compared with the findings of this systematic review. Thus, a color-coded bone model could help to achieve as good a postoperative ROM and MEPS for advanced elbow osteoarthritis as those for early and intermediate stages.

This study has some limitations. First, it was retrospective; thus, the patients' backgrounds differed regarding age, preoperative restricted extension, and severity of osteoarthritis. Second, the sample size was small for the 3 surgeons, which might result in variability in clinical outcomes. However, the results of this study suggest that even if group 2 includes patients with a preoperative arc $< 80^\circ$, which indicates a poor predicted outcome, the results are comparable to those of group 1. Precise resection of the impinging lesion using a color-coded bone model might be useful in achieving the range of extension, especially in severe cases. Finally, it would be appropriate to evaluate improvement in resection accuracy comparing preoperative and postoperative 3D CT scans. However, to avoid additional radiation exposure for patients, we did not postoperatively assess 3D CT scans in all cases; therefore, we could not evaluate the resection accuracy of the impinging lesion.

Conclusion

The color-coded 3D resin bone model made identifying the impinging region easy during arthroscopic arthroplasty for osteoarthritis of the elbow joint. We expect good results, especially in patients with severely restricted extension.

Disclaimer

Kunihiro Oka has received funding from the Japan Society for the Promotion of Science (KAKENHI grant no. JP18K12104). All the other authors, their immediate families, and any research foundations with which they are affiliated have not received any financial payments or other benefits from any commercial entity related to the subject of this article.

References

1. Adams JE, King GJ, Steinmann SP, Cohen MS. Elbow arthroscopy: indications, techniques, outcomes, and complications. J Am Acad Orthop Surg 2014;22:810-8. https://doi.org/10.5435/jaaos-22-12-810
2. Adams JE, Wolff LH III, Merten SM, Steinmann SP. Osteoarthritis of the elbow: results of arthroscopic osteophyte resection and capsulectomy. J Shoulder Elbow Surg 2008;17:126-31. https://doi.org/10.1016/j.jse.2007.04.005
3. Antuna SA, Morrey BF, Adams RA, O'Driscoll SW. Ulnohumeral arthroplasty for primary degenerative arthritis of the elbow: long-term outcome and complications. J Bone Joint Surg Am 2002;84-a:2168-73. https://doi.org/10.2106/00004623-200212000-00007
4. Dalal S, Bull M, Stanley D. Radiographic changes at the elbow in primary osteoarthritis: a comparison with normal aging of the elbow joint. J Shoulder Elbow Surg 2007;16:358-61. https://doi.org/10.1016/j.jse.2006.08.005
5. Galle SE, Beck JD, Burchette RJ, Harness NG. Outcomes of elbow arthroscopic osteocapsular arthroplasty. J Hand Surg 2016;41:184-91. https://doi.org/10.1016/j.jhsa.2015.11.018
6. Goto A, Moritomo H, Murase T, Oka K, Sugamoto K, Arimura T, et al. In vivo elbow biomechanical analysis during flexion: three-dimensional motion analysis using magnetic resonance imaging. J Shoulder Elbow Surg 2004;13:441-7. https://doi.org/10.1016/j.jse.2004.01.022
7. Goto A, Murase T, Moritomo H, Oka K, Sugamoto K, Yoshikawa H. Three-dimensional in vivo kinematics during elbow flexion in patients with lateral humeral condyle nonunion by an image-matching technique. J Shoulder Elbow Surg 2014;23:318-26. https://doi.org/10.1016/j.jse.2013.11.010
8. Ikegami T, Maehara Y. Transplantation: 3D printing of the liver in living donor liver transplantation. Nat Rev Gastroenterol Hepatol 2013;10:697-8. https://doi.org/10.1038/nrgastro.2013.195
9. Kamineni S, Hirahara H, Pomianowski S, Neale PG, O'Driscoll SW, ElAttrache N, et al. Partial posteromedial olecranon resection: a kinematic study. J Bone Joint Surg Am 2003;85:1005-11. https://doi.org/10.2106/00004623-200306000-00004
10. Kelly EW, Bryce R, Coghlan J, Bell S. Arthroscopic debridement without radial head excision of the osteoarthritic elbow. Arthroscopy 2007;23:151-6. https://doi.org/10.1016/j.arthro.2006.10.008
11. Krishnan SG, Harkins DC, Pennington SD, Harrison DK, Burkhead WZ. Arthroscopic ulnohumeral arthroplasty for degenerative arthritis of the elbow in patients under fifty years of age. J Shoulder Elbow Surg 2007;16:443-8. https://doi.org/10.1016/j.jse.2006.09.001
12. Kroonen LT, Piper SL, Ghatan AC. Arthroscopic management of elbow osteoarthritis. J Hand Surg 2017;42:640-50. https://doi.org/10.1016/j.jhsa.2017.05.023
13. Lim TK, Koh KH, Lee HI, Shim JW, Park MJ. Arthroscopic debridement for primary osteoarthritis of the elbow: analysis of preoperative factors affecting outcome. J Shoulder Elbow Surg 2014;23:1381-7. https://doi.org/10.1016/j.jse.2014.01.009
14. Miyake J, Murase T, Oka K, Moritomo H, Sugamoto K, Yoshikawa H. Computer-assisted corrective osteotomy for malunited diaphyseal forearm fractures. J Bone Joint Surg Am 2012;94:e150. https://doi.org/10.2106/jbjs.k.00829
15. Miyake J, Shimada K, Moritomo H, Kataoka T, Murase T, Sugamoto K. Kinematic changes in elbow osteoarthritis: in vivo and 3-dimensional analysis using computed tomographic data. J Hand Surg 2013;38:957-64. https://doi.org/10.1016/j.jhsa.2013.02.006
16. Miyake J, Shimada K, Oka K, Tanaka H, Sugamoto K, Yoshikawa H, et al. Arthroscopic debridement in the treatment of patients with osteoarthritis of the elbow, based on computer simulation. Bone Joint J 2014;96-b:237-41. https://doi.org/10.1302/0301-620x.96b2.30714
17. Mobbs RJ, Coughlan M, Thompson R, Sutterlin CE. The utility of 3D printing for surgical planning and patient-specific implant design for complex spinal pathologies: case report. J Neurosurg Spine 2017;26:513-8. https://doi.org/10.3171/2016.9.spine16371
18. Morrey BF. Primary degenerative arthritis of the elbow. Treatment by ulnohumeral arthroplasty. J Bone Joint Surg Br 1992;74:409-13.
19. Murase T, Oka K, Moritomo H, Goto A, Yoshikawa H, Sugamoto K. Three-dimensional corrective osteotomy of malunited fractures of the upper extremity with use of a computer simulation system. J Bone Joint Surg Am 2008;90:2375-89. https://doi.org/10.2106/jbjs.g.01299
20. O'Driscoll SW. Arthroscopic treatment for osteoarthritis of the elbow. Orthop Clin North Am 1995;26:691-706.
21. Oka K, Doi K, Suzuki K, Murase T, Goto A, Yoshikawa H, et al. In vivo three-dimensional motion analysis of the forearm with radioulnar synostosis treated by the Kanaya procedure. J Orthop Res 2006;24:1028-35. https://doi.org/10.1002/jor.20136
22. Oka K, Moritomo H, Goto A, Sugamoto K, Yoshikawa H, Murase T. Corrective osteotomy for malunited intra-articular fracture of the distal radius using a custom-made surgical guide based on three-dimensional computer simulation: case report. J Hand Surg 2008;33:835-40. https://doi.org/10.1016/j.jhsa.2008.02.008
23. Oka K, Tanaka H, Okada K, Sahara W, Myoui A, Yamada T, et al. Three-dimensional corrective osteotomy for malunited fractures of the upper extremity using patient-matched instruments: a prospective, multicenter, open-label, single-arm trial. J Bone Joint Surg Am 2019;101:710-21. https://doi.org/10.2106/jbjs.18.00765
24. Omori S, Murase T, Kataoka T, Kawanishi Y, Oura K, Miyake J, et al. Three-dimensional corrective osteotomy using a patient-specific osteotomy guide and bone plate based on a computer simulation system: accuracy analysis in a cadaver study. Int J Med Robot 2014;10:196-202. https://doi.org/10.1002/rcs.1530
25. Park JH, Lee Y, Shon OJ, Shon HC, Kim JW. Surgical tips of intramedullary nailing in severely bowed femurs in atypical femur fractures: simulation with 3D printed model. Injury 2016;47:1318-24. https://doi.org/10.1016/j.injury.2016.02.026
26. Perica ER, Sun Z. A systematic review of three-dimensional printing in liver disease. J Digit Imaging 2018;31:692-701. https://doi.org/10.1007/s10278-018-0067-x
27. Rettig LA, Hastings H II, Feinberg JR. Primary osteoarthritis of the elbow: lack of radiographic evidence for morphologic predisposition, results of operative debridement at intermediate follow-up, and basis for a new radiographic classification system. J Shoulder Elbow Surg 2008;17:97-105. https://doi.org/10.1016/j.jse.2007.03.014
28. Sarris I, Riano FA, Goebel F, Goitz RJ, Sotereanos DG. Ulnohumeral arthroplasty: results in primary degenerative arthritis of the elbow. Clin Orthop Relat Res 2004;420:190-3.
29. Sochacki KR, Jack RA II, Hirase T, McCulloch PC, Lintner DM, Liberman SR, et al. Arthroscopic debridement for primary degenerative osteoarthritis of the elbow leads to significant improvement in range of motion and clinical outcomes: a systematic review. Arthroscopy 2017;33:2255-62. https://doi.org/10.1016/j.arthro.2017.08.247
30. Stanley D. Prevalence and etiology of symptomatic elbow osteoarthritis. J Shoulder Elbow Surg 1994;3:386-9.
31. Steinmann SP, King GJ, Savoie FH III. Arthroscopic treatment of the arthritic elbow. J Bone Joint Surg Am 2005;87:2114-21. https://doi.org/10.2106/00004623-200509000-00026
32. Tsuge K, Mizuseki T. Debridement arthroplasty for advanced primary osteoarthritis of the elbow. Results of a new technique used for 29 elbows. J Bone Joint Surg Br 1994;76:641-6.
33. Wada T, Isogai S, Ishii S, Yamashita T. Debridement arthroplasty for primary osteoarthritis of the elbow. J Bone Joint Surg Am 2004;86:233-41. https://doi.org/10.2106/00004623-200402000-00004
34. Yang T, Lin S, Xie Q, Ouyang W, Tan T, Li J, et al. Impact of 3D printing technology on the comprehension of surgical liver anatomy. Surg Endosc 2019;33:411-7. https://doi.org/10.1007/s00464-018-6308-8
35. Zeng C, Xing W, Wu Z, Huang H, Huang W. A combination of three-dimensional printing and computer-assisted virtual surgical procedure for preoperative planning of acetabular fracture reduction. Injury 2016;47:2223-7. https://doi.org/10.1016/j.injury.2016.03.015